Published in final edited form as:
Biomaterials. 2014 March ; 35(10): 3220–3228. doi:10.1016/j.biomaterials.2013.12.087.

Reduction of ectopic bone growth in critically-sized rat mandible defects by delivery of rhBMP-2 from kerateine biomaterials

Christine J. Kowalczewski[a,b], **Seth Tombyln**[c], **David C. Wasnick**[a], **Michael R. Hughes**[d], **Mary D. Ellenburg**[c], **Michael F. Callahan**[e], **Thomas L. Smith**[f], **Mark E. Van Dyke**[g], **Luke R. Burnett**[c], and **Justin M. Saul**[a,*]

[a] Department of Chemical, Paper, and Biomedical Engineering, Miami University, 650 E. High St., Oxford, OH 45056, USA

[b] School of Biomedical Engineering and Sciences, Virginia Tech-Wake Forest University, Medical Center Blvd, Winston-Salem, NC 27157, USA

[c] KeraNetics, LLC, Richard Dean Biomedical Research Building, Suite 168, 391 Technology Way, Winston-Salem, NC 27101, USA

[d] Department of Statistics, Miami University, 311 Upham Hall, 501 E. High St., Oxford, OH 45056, USA

[e] Animal Health Specialties, LLC, MU Life Sciences Business Incubator at Monsanto Place, 1601 South Providence Road, Columbia, MO 65211, USA

[f] Department of Orthopaedic Surgery, Wake Forest University School of Medicine, Medical Center Boulevard, Winston-Salem, NC 27157, USA

[g] School of Biomedical Engineering and Sciences, Virginia Tech-Wake Forest University, 317 Kelly Hall, Stanger St, Blacksburg, VA 24061, USA

Abstract

Absorbable collagen sponges (ACS) are used clinically as carriers of recombinant human bone morphogenetic protein 2 (rhBMP-2) to promote bone regeneration. ACS exhibit ectopic bone growth due to delivery of supraphysiological levels of rhBMP-2, which is particularly problematic in craniofacial bone injuries for both functional and esthetic reasons. We hypothesized that hydrogels from the reduced form of keratin proteins (kerateine) would serve as a suitable alternative to ACS carriers of rhBMP-2. The rationale for this hypothesis is that keratin biomaterials degrade slowly *in vivo*, have modifiable material properties, and have demonstrated capacity to deliver therapeutic agents. We investigated kerateine hydrogels and freeze-dried

* Corresponding author. Department of Chemical, Paper, and Biomedical Engineering, 650 East High Street, Engineering Building, Room 064L, Miami University, Oxford, OH 45056, USA. Tel.: +1 513 529 0769; fax: +1 513 529 0761. sauljm@MiamiOH.edu (J.M. Saul)..

Conflicts of interest

Some authors have potential conflicts interest to disclose as co-founder (MEVD), shareholders (MEVD, LRB, MDE, ST), employees (LRB, MDE, ST), or received research/institutional support from KeraNetics LLC (JMS, MEVD, TLS, CJK). Wake Forest University Health Sciences has a potential financial interest in KeraNetics, LLC through licensing agreements. The terms of this arrangement have been reviewed and approved by Wake Forest University Health Sciences in accordance with its conflict of interest policy.

scaffolds as rhBMP-2 carriers in a critically-sized rat mandibular defect model. ACS, kerateine hydrogels, and kerateine scaffolds loaded with rhBMP-2 achieved bridging in animals by 8 weeks as indicated by micro-computed tomography. Kerateine scaffolds achieved statistically increased bone mineral density compared to ACS and kerateine hydrogels, with levels reaching those of native bone. Importantly, both kerateine hydrogels and kerateine scaffolds had significantly less ectopic bone growth than ACS sponges at both 8 and 16 weeks post-operatively. These studies demonstrate the suitability of keratins as rhBMP-2 carriers due to equal regenerative capacity with reduced ectopic growth compared to ACS.

Keywords

Bone regeneration; Collagen; Hydrogel; Scaffold; *In vivo* test; Keratin

1. Introduction

High-energy craniofacial trauma is seen in 75% motor vehicle accidents [1] and 29% of battlefield injuries from improvised explosive devices [2]. The resulting injuries are irregularly shaped and affect a number of tissues including muscle, nerve, and bone [3]. Irregularly shaped craniofacial bone injuries are often too large to heal spontaneously without external intervention (i.e., they are critically-sized). Over the past few years the number of maxillofacial reconstructive procedures has dramatically increased; with over 200,000 procedures performed in 2012 alone [4]. Complications arising from the use of auto and allogeneic bone grafts as well as the difficulty of their use in critically-sized bone defects in the head, face, and jaw have led to increased clinical interest in the use of bone substitutes [5].

Bone substitutes often incorporate potent exogenous agents such as recombinant human bone morphogenetic protein 2 (rhBMP-2) to recruit marrow and periosteal pre-osteoblasts to differentiate and bridge the defect site [6]. Exogenous delivery of rhBMP-2 requires a carrier system to overcome a short systemic half-life and prevent rapid diffusion of the rhBMP-2 away from the implant (injury) site. FDA-approved collagen-based rhBMP-2 carriers such as Medtronic's Infuse® have been successful in restricted applications, including maxillofacial bone grafts [7]. Unfortunately, the large dose of rhBMP-2 required to elicit a therapeutic response causes an over activation of osteogenic differentiation near the treatment area due to the effects of rhBMP-2 on preosteogenic cells of mesenchymal lineage found in the neighboring muscle and periosteum [8,9]. Further, the supraphysiological release of rhBMP-2 caused by the inability to retain the rhBMP-2 and the enzymatic degradation of the collagen sponge results in side effects in the surrounding area including ectopic bone growth, bone resorption, and edema [10,11]. Due to these clinically observed adverse events and the irregular geometry of craniofacial bone defects, it is clear that alternative carrier systems for rhBMP-2 are needed. Natural polymers are of particular interest as rhBMP-2 carriers because they are often bioresorbable, elicit limited immune response, have low cytotoxicity, and unlike synthetic polymers they can be cleared and metabolized by the host with minimal inflammatory response [12].

Keratins are intermediate filament proteins widely found in nature and are best known as being the structural proteins found in wool, hooves, and hair. Keratins are commonly extracted from wool and human hair because these are a renewable source for biomaterials. Although there are a number of keratinases produced by bacteria [13] and fungi [14], keratinase enzymes have not been identified in humans, making keratin biomaterials attractive for long-term drug delivery due to slow *in vivo* resorption. Keratins are also attractive as biomaterials and as carriers of rhBMP-2 because they are easily sterilized, are hydrolytically degraded, and have material properties that can be modified [15–17]. Modification of keratin's material properties is achieved through two general methods of extraction: oxidative or reductive. Each respective method leads to different material properties of the resulting processed biomaterials due to differences in the chemical nature of the cysteine residues that result from these extraction chemistries [18,19]. The oxidative form, keratose, lacks disulfide cross-links due to sulfonic acid residues on cysteine [16]. This results in a material that rapidly degrades; therefore, keratose was not used in the studies described in this manuscript. Kerateine, the form of keratin resulting from reductive extraction (see Fig. 1, step 1), acquires material properties from both physical entanglements and the formation of covalent disulfide bonds between cysteine residues (i.e., cystine), which results in a stable, crosslinked hydrogel [17]. Extracted keratin proteins (both keratose and kerateine) can be further processed to obtain two sub-fractions: alpha (α) keratin and gamma (γ) keratin. α-keratin is the key structural component due to its alpha-helical tertiary structure, and γ-keratin is a high sulfur containing globular protein (see Fig. 1, step 2) [20].

In the work reported here, we explored the use of kerateine (reductive extraction) as a carrier for rhBMP-2 as an alternative to absorbable collagen sponges for application to craniofacial defects. Our rationale was that the presence of disulfide bonds in kerateine (reductive form of keratin) would lead to *in vivo* stability on the order of months, which is a timescale appropriate for bone regeneration. Furthermore, we have previously observed, and confirmed in this report, a correlation between the rate of hydrogel degradation and the rate of therapeutic agent delivery [21,22]. For these reasons, we hypothesized that kerateine biomaterials could be properly formulated to support controlled delivery of rhBMP-2 that would improve measures of bone regeneration (bridging and bone mineral density) while reducing negative side effects (ectopic bone growth) associated with current clinically-used absorbable collagen sponges. We specifically investigated two types of kerateine carriers: (1) an injectable hydrogel and (2) an implantable (freeze-dried hydrogel) scaffold that was fabricated to the geometry of the defect. After initial characterization of mechanical, scaffold/gel degradation, and rhBMP-2 release, we then applied the kerateine carriers to a critically-sized rat mandibular defect model to assess measures of healing including bone regeneration and ectopic bone growth. We compared the kerateine biomaterials directly to the current clinical system of rhBMP-2 delivery from absorbable collagen sponges.

2. Materials and methods

2.1. rhBMP-2 carrier preparation

Lyophilized and sterile (via 2 MRad gamma-irradiation) kerateine powder (see Fig. 1, step 3) was obtained from KeraNetics, Winston-Salem, NC. Under sterile conditions, a 6%

(weight/volume) kerateine powder at an 80:20 ratio of α:γ kerateine (which we refer to as 6% 80:20 kerateine) was reconstituted in water with or without 100 μg/mL rhBMP-2 (Pfizer, New York, NY) (see Fig. 1, step 4). The mixture was then vortexed, centrifuged, and incubated overnight at 37 °C to form gels. Kerateine scaffolds were formed by freeze-drying 5 mm circular biopsy punches of hydrogels of a thickness of 2.5 mm (see Fig. 1, step 5). 5 μg of rhBMP-2 was present in each kerateine gel or scaffold used for *in vitro* and *in vivo* experiments. 5 mm diameter absorbable collagen sponges (ACS) were obtained from an XX-small Infuse kit (Medtronic, Minneapolis, MN) by biopsy punch. 5 μg total rhBMP-2 was loaded onto each ACS. This is consistent with manufacturer's recommended method of preparation with the exception of a reduced rhBMP-2 dosage and scaffold size.

2.2. Scanning electron microscopy

Lyophilized kerateine scaffolds were gold sputter coated (Denton Desk II Cold Sputter Coater, Moorestown, NJ) and imaged at 5000× magnification with a Zeiss Supra 35VP FEG SEM (Oberkochen, Germany).

2.3. Rheology

A 6% 80:20 kerateine powder in water without rhBMP-2 was vortexed, centrifuged, loaded into a 22 × 1.2 mm cylindrical teflon template, and then incubated overnight at 37 °C to make a homogenous gel ($n = 3$). Samples were then loaded onto a Bohlin CS-10 Rotational Rheometer (Malvern, Worcestershire, UK) system with parallel plate geometry (gap width = 1 mm) for assessment of gel rheological characteristics at room temperature (25 °C). A dynamic oscillation stress sweep at a constant frequency of 1 Hz was used to determine the linear viscoelastic region (LVER) of the kerateine biomaterial. A frequency sweep from 0.1 to 10 Hz was then performed at a constant stress (25 kPa) within the LVER.

2.4. In vitro rhBMP-2 carrier characterization

Release of rhBMP-2 from each carrier was determined *in vitro* over the course of 4 weeks. rhBMP-2 carriers (kerateine gel, kerateine scaffold, or absorbable collagen sponge) loaded with 5 μg rhBMP-2 were prepared as described above and placed in a 1.5 mL conical tube. Data show the results of a single experiment ($n = 3$) that was conducted twice. Carriers without rhBMP-2 served as negative controls. 100 μL of sterile PBS (Gibco, Grand Island, NY) was added to each conical tube. Tubes were then incubated at 37 °C. At pre-assigned time points the PBS was removed and replaced with fresh 100 μL PBS. Collected samples were frozen at –80 °C until analysis was performed by DC Protein Assay (Bio-Rad, Hercules, CA) for carrier degradation and rhBMP-2 ELISA (Peprotech, Rocky Hill, NJ) for rhBMP-2 release.

2.5. Critically-sized rat mandible defect model

All animal studies were conducted with the approval and guidance of the Miami University Institutional Animal Care and Use Committee (IACUC). 350 g male Sprague Dawley rats (Harlan, Indianapolis, IN) that were approximately 10 weeks old were anesthetized with isoflurane. Under aseptic conditions, an incision was made through the masseter muscle, which was retracted to expose the bone of the masseteric fossa. A full thickness 5 mm

diameter circular critically-sized defect was created with a sterile 2.4 mm circular engraving cutter (Dremel, Racine, WI) with intermittent rinses of PBS (Gibco, Grand Island, NY). The defect was then treated with carriers either containing or lacking 5 μg rhBMP-2. The ACS and kerateine scaffolds were placed directly into the surgical defect site while kerateine hydrogels were injected from a sterile 1 mL syringe. After application of treatment groups, the masseter muscle held the treatment in place and was closed with resorbable POLYSORB suture (Syneture, Norwalk, CT). The skin was closed with nonresorbable SURGIPRO suture (Syneture, Norwalk, CT) and was removed one week later. Control animals receiving "no treatment" were closed without implanting or injecting materials to the mandibular defect. Five animals with bilateral defects (10 total defects) were used per treatment group. Five animals that did not undergo the surgical procedure served as controls for normal, age-matched bone.

2.6. μCT image analysis of bone regeneration and ectopic growth

Non-invasive assessment of *in vivo* bone regeneration was determined by 52 micron resolution (voxel size 0.00014 mm^3) micro-Computed Tomography (μCT) (Imtek MicroCAT II, Siemens, USA) in the Imaging Research Center at the Cincinnati Children's Hospital Medical Center at 8 and 16 weeks post-operatively. μCT images were reconstructed in Osirix DICOM-viewer (Pixmeo, Geneva, Switzerland) with 3D surface rendering (Osirix threshold for bone = 625 pixel). When un-bridged defector ectopic growth was observed, regions of interest (ROI) were drawn around respective boundaries on every tenth image and interpolated to obtain volume renderings of the defect or ectopic growth. Percent bone regeneration was calculated by normalizing the volume of the un-bridged defect ROI by the original defect volume. Bone mineral density of treatment area was calculated from known gray scale standards run with each μCT scan and determined by gray scale analysis in ImageJ (NIH, USA). Bone mineral density of regenerated tissue within the defect area was normalized to the bone mineral density of controls of normal, age-matched bone of the masseteric fossa.

2.7. Tissue processing and staining

After the 16 week μCT scan, rats were humanely euthanized. The mandibles were immediately harvested and hemi-mandibles separated. Tissue was fixed for three days in 10% neutral buffer formalin (Shandon Formal Fix, Thermo Scientific, Waltham, MA), decalcified for three days in formic acid (Immunocal, Decal Chemical Corporation, Tallman, NY), and decalcification stopped with Cal-Arrest (Decal Chemical Corporation, Tallman, NY). Tissue was then soaked in PBS for 3 days, placed in 30% sucrose overnight, and embedded in paraffin. Tissue was sectioned in the coronal plane by microtome (Microm HM 355s, Thermo Scientific, Florence, KY) into 10 μm sections on positively charged slides (Leica, DE). After drying overnight at 60 °C, slides were stained with Masson's Trichrome (American Master Tech, Lodi, CA). Slides were imaged with a 4× objective on an AX70 Olympus (Center Valley, PA) microscope and images captured with a Nikon D300 (Tokyo, Japan). Due to the size of the defect, multiple images of each respective defect were combined to form panoramic images by using Adobe Elements (Adobe Systems, San Jose, CA).

2.8. Statistical analysis

In vitro data was analyzed by using one-way analysis of variance (ANOVA) with Tukey's post-hoc comparisons. *In vivo* analysis of bone regeneration, bone mineral density, and ectopic bone growth was performed by using mixed model ANOVA with planned post-hoc comparison using Bonferroni correction. An arcsine transformation was applied to the percent bone regeneration prior to model fitting to stabilize variance. Statistically significant *p*-values are presented in both the text and figure legends. Analyses were performed by using Minitab version 16 (Minitab, State College, PA) or SAS® version 9.2 for Windows (SAS Institute, Cary, NC).

3. Results

3.1. Scanning electron microscopy

Several kerateine formulations were tested for rheology and degradation profiles to determine a material that would have suitable mechanical and degradation properties (data not shown). We report on the final formulation selected, which was 6% kerateine (w/v) for a hydrogel with an 80:20 ratio of α:γ. Fig. 1B shows an SEM image of the resulting freeze-dried scaffold material for this formulation, demonstrating the porous nature of the materials.

3.2. Rheology

Kerateine hydrogel physical characteristics were determined by oscillatory rheology within the LVER. Kerateine material properties can be modified by either weight percent or the ratio of alpha to gamma kerateine in the material formulation. At a constant shear stress (τ = 25 Pa) a frequency sweep from 0.1 to 10 Hz shows little effect on the complex modulus of the hydrogel (Fig. 2). The elastic modulus (G') is greater than the viscous modulus (G''), the phase angle (°) is close to 0°, and tan δ is less than 1 along the frequency sweep. These findings are indicative of formation of a stable crosslinked hydrogel network showing characteristics of an elastic solid gel.

3.3. In vitro rhBMP-2 carrier characterization

Analysis of carrier degradation showed that both the kerateine gel and scaffold at the initial time point (1.5 h of incubation) had 10.0% of the total protein erode from each of the carriers (Fig. 3A). At the end of the four week period the kerateine gel had the greatest cumulative erosion (32.4 ± 3.2%) followed by the kerateine scaffold (23.7 ± 1.9%) while the ACS had the least cumulative erosion (17.1 ± 1.2%). rhBMP-2 release was measured over a four week period to compare kerateine gels, kerateine scaffolds, and ACS carriers. To observe if rhBMP-2 kerateine carriers have an initial burst release like ACS, a rhBMP-2 release kinetic study was pre-formed (Fig. 3B). Linear regression over initial (linear) release period of two days showed that ACS had a cumulative release of 6.8% of total rhBMP-2 per day whereas kerateine scaffolds released 3.0% of rhBMP-2 per day and kerateine gels released 2.3% of rhBMP-2 per day. The initial rate of rhBMP-2 release from kerateine gels and scaffolds demonstrated 66.0% and 55.0% lower rhBMP-2 release rates, respectively, compared to ACS when measuring the linear regression over the first two days. The

kerateine gel had a 25.0% lower rate of rhBMP-2 release compared to the kerateine scaffold. The greatest total rhBMP-2 release over the total 4 week period was from the ACS (32.1 ± 2.6%) followed by the kerateine scaffolds (15.9 ± 1.2%). If the initial 6.0% burst release at the first time point (1.5 h) after rehydration of the kerateine scaffolds is subtracted, then the kerateine scaffolds show a release profile similar to kerateine gels (8.0 ± 0.7%).

3.4. Bone regeneration and ectopic bone growth analysis

μCT images of bone regeneration 16 weeks after surgical creation of bilateral 5 mm critically-sized circular mandibular defects (Fig. 4A) were compared to μCT reconstruction of normal mandibular bone (Fig. 4B). 3D renderings of μCT images indicate that untreated rat mandibles (Fig. 4C) as well as those treated with kerateine gels (Fig. 4E) or scaffolds (Fig. 4G) without rhBMP-2 did not spontaneously heal by 16 weeks, highlighting the critical-sized nature of the defect. In contrast, 3D reconstruction of week 16 μCT images demonstrates the ability of ACS (Fig. 4D), injectable kerateine gels (Fig. 4F) and scaffolds (Fig. 4H) loaded with rhBMP-2 to elicit complete bridging of the defect.

Measurements of defect volumes show that, at 8 and 16 weeks, groups not treated with rhBMP-2 resulted in statistically less bone regeneration compared to rhBMP-2 treated groups (Fig. 5A). Interestingly, kerateine gels alone (without rhBMP-2) were able to achieve statistically more bone regeneration than no treatment and scaffold only after 16 weeks. rhBMP-2 carriers (ACS, kerateine gel, and kerateine scaffold) were statistically equivalent to one another and were able to bridge the defect gap after 8 weeks (Fig. 5A, 8 week data).

Differentiation between cartilaginous and bone tissue was determined by thresholding the μCT images as well as measuring the bone mineral density (BMD) within the defect area (Fig. 5B). At 8 and 16 weeks, treatment groups without rhBMP-2 had statistically lower BMD than normal bone and rhBMP-2 carrier groups. Kerateine rhBMP-2 loaded gels performed statistically as well as the ACS carriers at 8 weeks and had statistically greater BMD by 16 weeks. Kerateine scaffolds loaded with rhBMP-2 achieved statistically greater BMD than ACS at both time points. More importantly, the kerateine scaffold rhBMP-2 carrier was the only treatment group to achieve BMD values that were statistically equivalent to normal, uninjured, age-matched bone.

Reconstruction of DICOM images revealed formation of ectopic bone growth in all experimental groups containing rhBMP-2, as shown by arrowheads in Fig. 4D, F and H. Groups not treated with rhBMP-2 (no treatment Fig. 4C; kerateine gel Fig. 4E; and kerateine scaffold Fig. 4G) showed no evidence of ectopic growth. Quantification of ectopic growth in rhBMP-2 treated animals was measured by using Osirix 3D volume rendering. As can be observed in Fig. 4D, F and H and quantified in Fig. 6, kerateine gels and scaffolds used as carriers for rhBMP-2 had significantly less ectopic growth than ACS at the same rhBMP-2 dose at both 8 and 16 week measurements.

3.5. Histology

Histological evaluation of experimental treatment groups was performed in order to evaluate the regenerated tissue within the defect site (Fig. 7). Masson's trichrome stains mature bone matrix and endogenous keratin (intracellular not from implanted materials) red while fibrous

tissue, osteoid, and collagenous tissue stain blue. Differences in observed defect area (dashed and solid lines) are a result of taking images at different areas along the defect site. No treatment (Fig. 7B), kerateine scaffold (no rhBMP-2; Fig. 7C) and kerateine gel (no rhBMP-2; Fig. 7D) showed clear defect boundaries with infiltration of soft collagen matrix (dashed line). Kerateine, which was not fully degraded and remains brown in color, can be seen in the middle of the defect area in both kerateine gel and scaffolds not loaded with rhBMP-2 (Fig. 7C and D highlighted by black arrow within insets). All rhBMP-2 carrier groups (ACS, Fig. 7F; kerateine scaffold, Fig. 7G; and kerateine gel, Fig. 7H) showed bridging of the defect site with newly formed trabecular (T), woven (W), and mature (M) bone.

4. Discussion

There is a lack of suitable rhBMP-2 biomaterial carriers for the treatment of bone defects in the head, face, and jaw. The goal of these studies was to investigate the suitability of kerateine hydrogels or scaffolds as alternative carriers for rhBMP-2 in craniofacial or mandibular bone defects. The primary functions of BMP-2 carriers are (1) to increase the efficacy of rhBMP-2 by preventing rapid diffusion away from the injury site while promoting a chemo-attractive gradient and (2) to provide a matrix for migrating cells.

From the *in vitro* rhBMP-2 release studies, even though the ACS does not hydrolytically erode as quickly as the kerateine carriers, it does have a greater release of rhBMP-2. There is a strong positive correlation between high protein isoelectric points (rhBMP-2 pI ~ 8.5) and retention times within a carrier system [10,23] with mild acidic conditions [24]. Because keratin has an isoelectric range less than neutral (pH 5–6, where range indicates that multiple keratin protein are present) [19], it can immobilize molecules with opposite charge (at neutral pH) such as rhBMP-2. This may explain why the rhBMP-2 release plateaus after five days compared to collagen (pI ~ 8.26) [25], which continues a steady release of rhBMP-2 *in vitro*. After the initial release of soluble rhBMP-2 was observed for both the kerateine gel and scaffold, release plateaued after the third day suggesting the remainder of the rhBMP-2 remains within the kerateine carrier matrix. It is important to note that this *in vitro* behavior will likely be different than *in vivo* behavior in regards to carrier degradation and thus rhBMP-2 release. Mammals are known to express collagenase enzymes that will degrade ACS sponges in several weeks. This would lead to rapid resorption of the ACS, causing subsequent increased release of rhBMP-2. This rapid resorption of collagen would lead to loss of the provisional matrix provided by the material, likely causing the commonly observed voids within the new bone matrix which is confirmed with our histological findings (Fig. 7F) [26,27]. In contrast, we are not aware of the presence of keratinase enzymes that specifically degrade keratins in mammals, indicating that the mechanism of keratin degradation *in vivo* would be hydrolytic and/or non-specific proteolytic degradation. This would lead to a more sustained rhBMP-2 release *in vivo* and longer time frame for the kerateine carrier to serve as a matrix to support infiltration of bone matrix forming cells. This is supported by histological images, which show the presence of implanted (not endogenous) kerateine materials at the defect site after 16 weeks *in vivo* (Fig. 7C and D insets).

While both ACS and kerateine gels or scaffolds loaded with rhBMP-2 led to bridging of the critically-sized gap, only kerateine scaffolds with rhBMP-2 led to bone mineral densities statistically equivalent to native bone by the 16 week time point. The presence of trabecular, woven, and mature bone observed in groups treated with rhBMP-2 carriers (kerateine and ACS) clearly indicates that the rhBMP-2 remained bioactive (osteoinductive) after biomaterial preparations.

Importantly, there was a significant difference in the levels of ectopic bone growth between the two carrier systems (ACS vs kerateine). This was grossly evident upon explantation of the jaws for tissue recovery and histology as large amounts of ectopic growth with the collagen carrier was readily observed. Ectopic growth is also demonstrated by both qualitative (Fig. 4D vs F and H; Fig. 7F vs G and H) and quantitative (Fig. 6) analysis of μCT scans and histological images. It might be argued that a lower dose of rhBMP-2 would have reduced the ectopic growth seen from the ACS sponges (as well as kerateine gels and scaffolds). However, we used a consistent dosage (5 μg of rhBMP-2 per defect site) that is in the range reported by other groups working in rat models [28,29]. This is an important result in that kerateine carriers (gels and scaffolds) of rhBMP-2 led to equivalent or better bone regeneration characteristics (bridging, bone volume, and bone mineral density) while at the same time achieving a significant reduction in ectopic bone growth compared to the ACS. We also note that in a previous study using oxidative form of keratin (keratose) similar levels of bone regeneration were achieved compared to ACS, but there were no observable differences in ectopic growth. However, in the current study using the reductive form of keratin (kerateine), similar levels of bone regeneration were achieved compared to ACS, but there was a significant reduction in ectopic growth. Although the animal models are different, this indicates a potential role for the form of the keratin carrier in controlling rhBMP-2 release and ectopic bone formation.

The histological evidence underscores the role that rhBMP-2 plays as an osteoinductive protein in bone regeneration but also highlights the less-appreciated role of the carrier. Location of osteoids in regions within the woven and mature bone matrix suggests active bone remodeling within all rhBMP-2 carrier groups (Fig. 7F, G, and H insets). These findings are indicative of the repair phase of bone healing seen in the first few months after injury. In the absence of rhBMP-2, defect sites treated with kerateine carriers alone did not calcify the collagenous tissue. The main issue with ACS is the initial increased release rate of a supraphysiological dose of rhBMP-2 into the local environment, which leads to ectopic bone growth [30]. This initial release would not be an issue with physiologically relevant levels of rhBMP-2, but in order to reach the therapeutic threshold current clinical applications use rhBMP-2 concentrations that are 10–1000 fold higher than native (endogenous) levels of BMP-2 [31]. The rate of biomaterial degradation is important not only for providing a structure for an appropriate length of time (in this case months) but also for controlling drug release. Equally important is the prevention of rapid rhBMP-2 diffusion away from the injury site, which promotes osteogenic cell proliferation and differentiation within the defect area.

It has been recently suggested that an initial burst release followed by a more sustained release of rhBMP-2 promotes more favorable bone healing [30]. Taken together, our results

suggest such a mechanism occurs in which kerateine carriers are able to promote more favorable mandibular bone regeneration with reduced ectopic growth. The relative lack of burst release by kerateine gels and scaffolds, compared to ACS, is sufficient to initiate bone healing but low enough to ultimately reduce levels of ectopic growth. From the *in vitro* data, it is clear that a large fraction of rhBMP-2 remains within the kerateine carrier. Therefore, there would be less of a diffusional gradient away from the carrier, leading to less differentiation of mesenchymal or muscle progenitor cells near but outside the carrier as a result of reduced levels of soluble rhBMP-2, thereby reducing ectopic bone growth [32]. This conclusion is supported by our observation during explant of the mandibles where the ectopic growth around ACS carriers had a gradient appearance ranging from bone closer to the implant site to more cartilaginous tissue further away from the implant, as would be expected from a decreasing rhBMP-2 gradient [33]. We also note that ectopic bone formation for ACS groups was aligned with the direction and location of the surgical incision, indicating that the ACS does not sequester the rhBMP-2 to the intended site of action. In other words, it is possible that the rhBMP-2 retained by the carrier is equally important to regeneration in the defect site as the soluble rhBMP-2 released from the carrier.

The result of similar or improved bone regeneration in combination with the reduced ectopic bone growth observed when using kerateine carriers is particularly important in craniofacial applications where it essential to preserve the esthetics of the facial structure by limiting ectopic bone formation. The tunable nature of kerateine formulations (e.g., by weight percent or α:γ ratios) lends itself to tailoring formulations to specific needs for a particular injury (e.g., rapid or sustained matrix degradation/rhBMP-2 delivery).

5. Conclusion

Kerateine biomaterials offer a naturally-based polymeric system that can provide tailored rhBMP-2 release profiles and degradation. In a critically-sized rat mandibular model the kerateine biomaterials reduced ectopic bone growth, and achieved comparable levels of bone healing to existing collagen-based clinical alternatives for mandible injuries. In addition, fabrication of rhBMP-2 carriers into easily deliverable injectable hydrogels or implantable scaffolds such as the kerateine carriers described in this report would reduce the invasive nature of reconstructive procedures, thereby reducing potential subsequent complications such as infection. The benefit of an injectable gel is the potential to conform directly to the irregularly shaped defect or a mold that fits the geometry of the craniofacial injuries. Given the challenges related to ectopic bone formation observed with ACS, the analogous healing profiles and reduction in ectopic bone formation observed with keratin-based carriers highlight the potential clinical utility of these materials in bone regeneration.

Acknowledgments

rhBMP-2 used for this work was generously donated by Pfizer. We acknowledge Cincinnati Children's Hospital Medical Center (Ronald Pratt, John Pearce, and Diana Lindquist) for μCT imaging and the Center for Applied Microscopy and Imaging (Richard Edelmann and Matthew Duley) for histological and SEM imaging. This work was partially supported by the National Institutes of Health (JMS; R01AR061391) and the content is solely the responsibility of the authors and does not necessarily represent the official views of the National Institutes of Health. This work was also partially supported by the US Army Medical Research and Materiel Command under Contract No.W81XWH-10-C-0165 (LB). The views, opinions and/or findings contained in this report are those of

the author(s) and should not be construed as an official Department of the Army position, policy or decision unless so designated by other documentation.

References

1. Katzen JT, Jarrahy R, Eby J, Mathiasen R, Margulies D, Shahinian H. Craniofacial and skull base trauma. J Trauma Injury Infect Crit Care. 2003; 54:1026–34.
2. Lew TA, Walker JA, Wenke JC, Blackbourne LH, Hale RG. Characterization of craniomaxillofacial battle injuries sustained by United States service members in the current conflicts of Iraq and Afghanistan. J Oral Maxillofac Surg. 2010; 68:3–7. [PubMed: 20006147]
3. Salinas NL, Brennan J, Gibbons MD. Massive facial trauma following improvised explosive device blasts in Operation Iraqi Freedom. Otolaryngol Head Neck Surg. 2011; 144:703–7. [PubMed: 21493311]
4. American Society of Plastic Surgeons. Plastic surgery procedural statistics. 2013. 2012 Online. Available from: URL:, http://www.plasticsurgery.org/Documents/news-resources/statistics/2012-Plastic-Surgery-Statistics/Cosmetic-Procedure-Trends-2012.pdf
5. Cutter CS, Mehrara BJ. Bone grafts and substitutes. J Long Term Eff Med Implants. 2006; 16:249–60. [PubMed: 17073567]
6. Wegman, F.; Geuze, RE.; Van Der Helm, YJ.; Öner, FC.; Dhert, WJA.; Alblas, J. Gene delivery of bone morphogenetic protein-2 plasmid DNA promotes bone formation in a large animal model.. Online J Tissue Eng Regen Med. Available from: URL:, http://onlinelibrary.wiley.com/doi/10.1002/term.1571/abstract; 2012 August
7. Mckay WF, Peckham SM, Badura JM. A comprehensive clinical review of recombinant human bone morphogenetic protein-2 (INFUSE® Bone Graft). Int Orthop. 2007; 2:729–34. [PubMed: 17639384]
8. Bosch P, Musgrave D, Lee JY, Cummins J, Shuler F, Ghivizzani S, et al. Osteo-progenitor cells in skeletal muscle. J Orthop Res. 1999; 18:933–44. [PubMed: 11192254]
9. Chappuis V, Gamer L, Cox K, Lowery JW, Bosshardt DD, Rosen V. Periosteal BMP2 activity drives bone graft healing. Bone. 2012; 51:800–9. [PubMed: 22846673]
10. Kempen DHR, Lu L, Hefferan TE, Creemers LB, Maran A, Classic KL, et al. Retention of in vitro and in vivo BMP-2 bioactivities in sustained delivery vehicles for bone tissue engineering. Biomaterials. 2008; 29:3245–52. [PubMed: 18472153]
11. Woo EJ. Adverse events reported after the use of recombinant human bone morphogenetic protein 2. J Oral Maxillofac Surg. 2012; 70:765–7. [PubMed: 22177811]
12. Ratner, BD.; Hoffman, AS.; Schoen, FJ.; Lemons, JE. Biomaterials science: an introduction to materials in medicine. 3rd ed.. Elsevier Inc.; Walham, MA: 2012.
13. Kumar R, Balaji S, Uma TS, Mandal AB, Sehgal PK. Optimization of influential parameters for extracellular keratinase production by Bacillus subtilis (MTCC9102) in solid state fermentation using horn meal – a biowaste management. Appl Biochem Biotechnol. 2010; 160:30–9. [PubMed: 19082924]
14. Anitha TS, Palanivelu P. Purification and characterization of an extracellular keratinolytic protease from a new isolate of Aspergillus parasiticus. Protein Expr Purif. 2013; 88:214–20. [PubMed: 23337085]
15. Rouse JG, Van Dyke ME. A review of keratin-based biomaterials for biomedical applications. Materials. 2010; 3:999–1014.
16. de Guzman RC, Merrill MR, Richter JR, Hamzi RI, Greengauz-Roberts OK, Van Dyke ME. Biomaterials mechanical and biological properties of keratose bio-materials. Biomaterials. 2011; 32:8205–17. [PubMed: 21835462]
17. Hill P, Brantley H, Van Dyke M. Some properties of keratin biomaterials: kerateines. Biomaterials. 2010; 31:585–93. [PubMed: 19822360]
18. Koehn H, Clerens S, Deb-Choudhury S, Morton JD, Dyer JM, Plowman JE. The proteome of the wool cuticle. J Proteome Res. 2010:2920–8. [PubMed: 20423113]
19. Plowman JE. The proteomics of keratin proteins. J Chromatogr. 2007; 849:181–9.

20. Crewther, WG.; Fraser, DB.; Lennox, FG.; Lindley, H. Advances in protein chemistry. Vol. 20. Academic Press; New York, NY: 1965. p. 191-347.
21. Saul JM, Ellenburg MD, de Guzman RC, Van Dyke M. Keratin hydrogels support the sustained release of bioactive ciprofloxacin. J Biomed Mater Res A. 2011; 98:544–53. [PubMed: 21681948]
22. de Guzman RC, Saul JM, Ellenburg MD, Merrill MR, Coan HB, Smith TL, et al. Bone regeneration with BMP-2 delivered from keratose scaffolds. Biomaterials. 2013; 34:1644–56. [PubMed: 23211447]
23. Uludag Hasan, Gao T. Delivery systems for BMPs: factors contributing to protein retention at an application site. J Bone Jt Surg. 2001:83–A.
24. Luca L, Rougemont A-L, Walpoth BH, Gurny R, Jordan O. The effects of carrier nature and pH on rhBMP-2-induced ectopic bone formation. J Control Release. 2010; 147:38–44. [PubMed: 20600403]
25. Zhang Z, Li G, Shi BI, Key T, Chemistry L. Physicochemical properties of collagen, gelatin and collagen hydrolysate derived from bovine limed split wastes. J Soc Leath Tech Ch. 2005; 90:23–8.
26. Friess W, Uludag H, Foskett S, Biron R, Sargeant C. Characterization of absorbable collagen sponges as rhBMP-2 carriers. Int J Pharm. 1999; 187:91–9. [PubMed: 10502616]
27. Gorham SD, Hyland TP, French DA, Willins MJ. Cellular invasion and breakdown of three different collagen films in the lumbar muscle of the rat. Bio-materials. 1990; 11:113–8.
28. Arosarena O, Collins W. Comparison of BMP-2 and -4 for rat mandibular bone regeneration at various doses 1. Orthod Craniofac Res. 2005; 8:267–76. [PubMed: 16238607]
29. Wen B, Karl M, Pendrys D, Shafer D, Freilich M, Kuhn L. An evaluation of BMP-2 delivery from scaffolds with miniaturized dental implants in a novel rat mandible model. J Biomed Mater Res Part B. 2011; 97B:315–26.
30. Brown KV, Lon M, Li B, Ph D, Guda T, Perrien DS, et al. Improving bone formation in a rat femur segmental defect by controlling bone morphogenetic protein-2 release. Tissue Eng Part A. 2011; 17:1735–46. [PubMed: 21338268]
31. Vaibhav B, Nilesh P, Vikram S, Anshul C. Bone morphogenic protein and its application in trauma cases: a current concept update. Injury. 2007; 38:1227–35. [PubMed: 17307180]
32. Katagiri T, Yamaguchi A, Komaki M, Abe E, Takahashi N, Ikeda T, et al. Bone morphogenetic protein-2 converts the differentiation pathway of C2C12 myoblasts into the osteoblast lineage. J Cell Biol. 1994; 127:1755–66. [PubMed: 7798324]
33. Puleo DA. Dependence of mesenchymal cell responses on duration of exposure to bone morphogenetic protein-2 in vitro. J Cell Physiol. 1997; 173:93–101. [PubMed: 9326453]

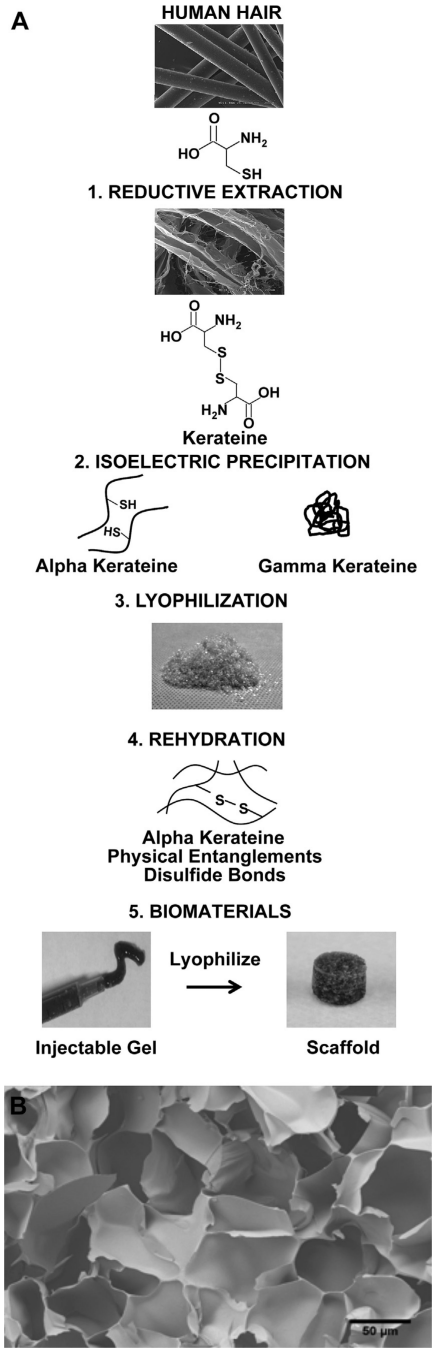

Fig. 1.

(A) Reductive extraction of human hair results in the reduced form of keratin known as kerateine. Further purification separates α and γ fractions of the kerateine extracts which can be freeze-dried and reconstituted to form a number of biomaterials including injectable hydrogels, which can be further processed into freeze-dried scaffolds (SEM images of hair reproduced with permission from de Guzman et al. [16]). (B) FE-SEM internal structure of a kerateine scaffold at 250× magnification.

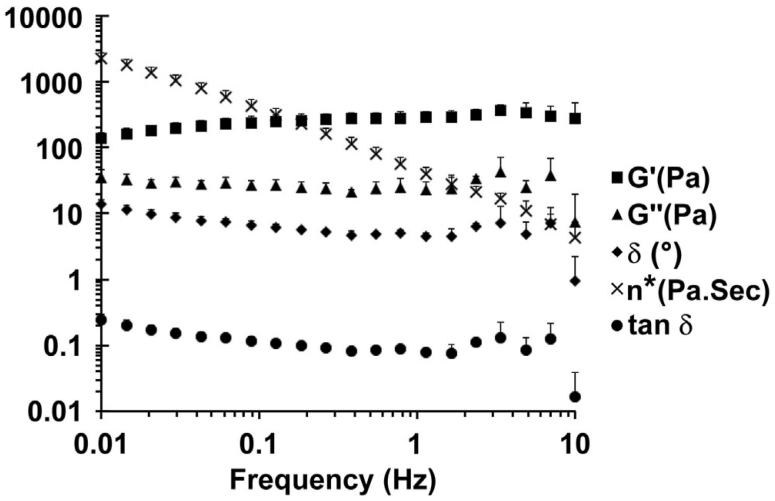

Fig. 2.

6% 80:20 kerateine hydrogel in the LVER acting with the typical behavior of a stable hydrogel network where G′ and G″ are independent of frequency and tan δ is close to 0 (Experimental $n = 3$, Mean ± SD).

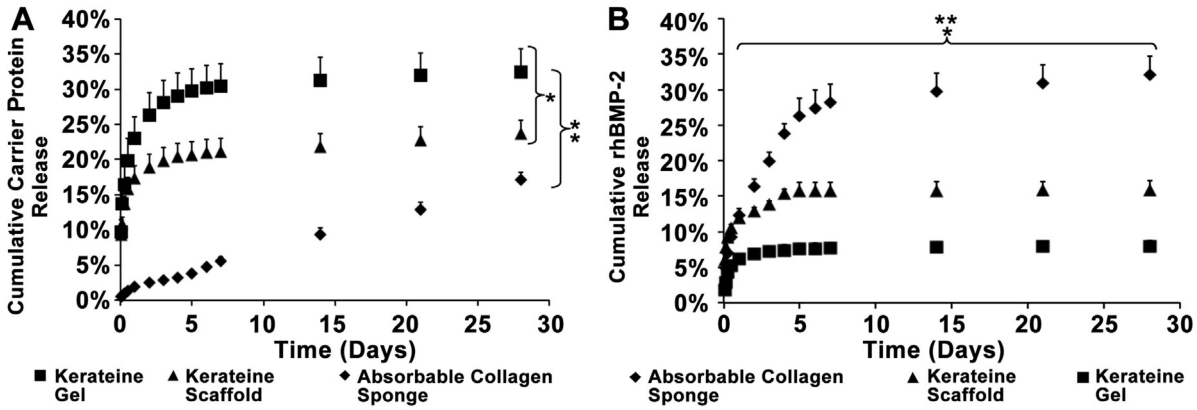

Fig. 3.

(A) Percentage of cumulative carrier erosion and (B) rhBMP-2 release from kerateine gel, kerateine scaffold, or ACS loaded with 5 μg of rhBMP-2 over a period of 4 weeks. Pairwise statistical comparisons were made between each group. (Experimental $n = 3$ Mean ± SD; *$p < 0.05$ kerateine gel vs kerateine scaffold, **$p < 0.05$ for both kerateine carriers vs ACS.)

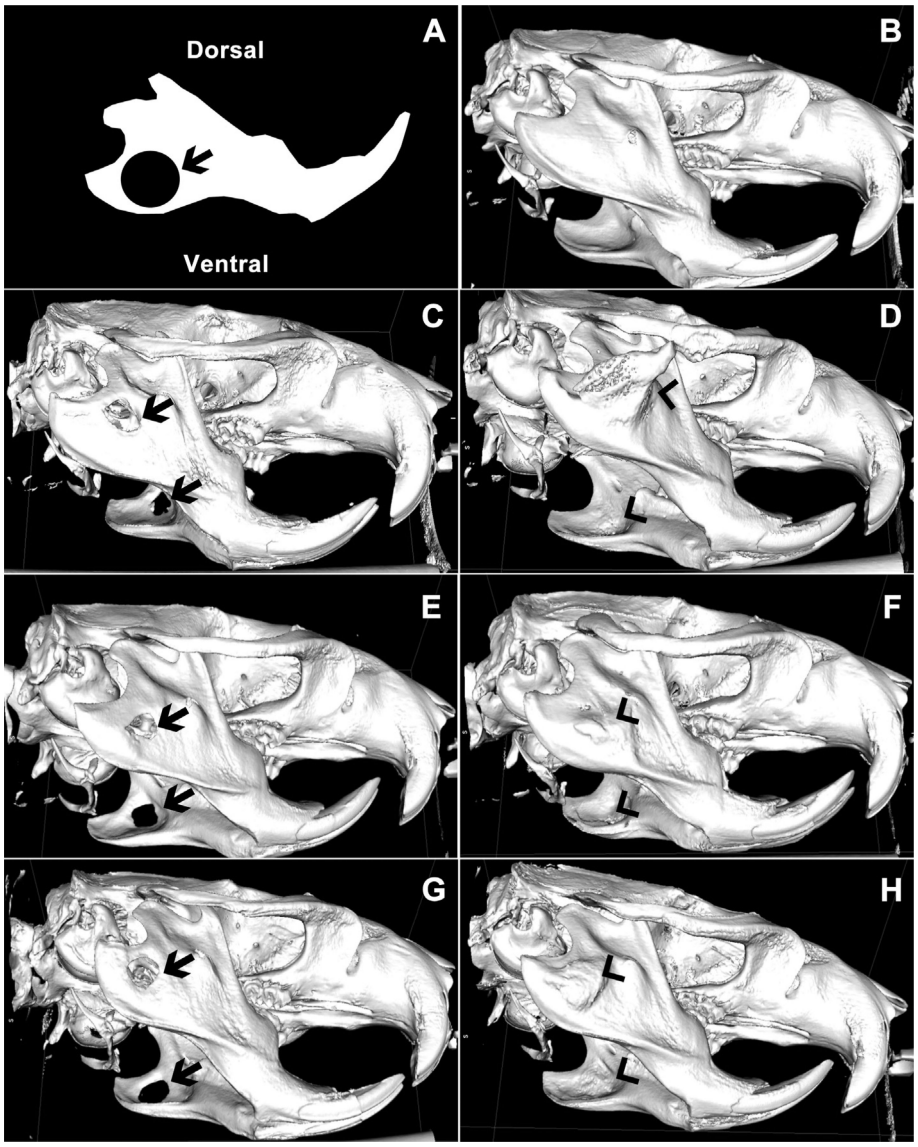

Fig. 4.

(A) Schematic of initial 5 mm defect size and location imposed on a sketch of a normal rat mandible. (B–H) Representative μCT images of bone regeneration sixteen weeks after surgical creation of a bilateral 5 mm critically-sized circular mandibular defect in (B) normal, uninjured, age-matched mandible, (C) rats receiving no treatment, (E) kerateine gel without rhBMP-2 or (G) kerateine scaffold without rhBMP-2 were unable to bridge the defect (arrows). Administration of (D) ACS with 5 μg rhBMP-2, (F) kerateine gel with 5 μg rhBMP-2, or (H) kerateine scaffold with 5 μg rhBMP-2 were able to close the defect with varying degrees of undesired ectopic bone growth (arrowheads).

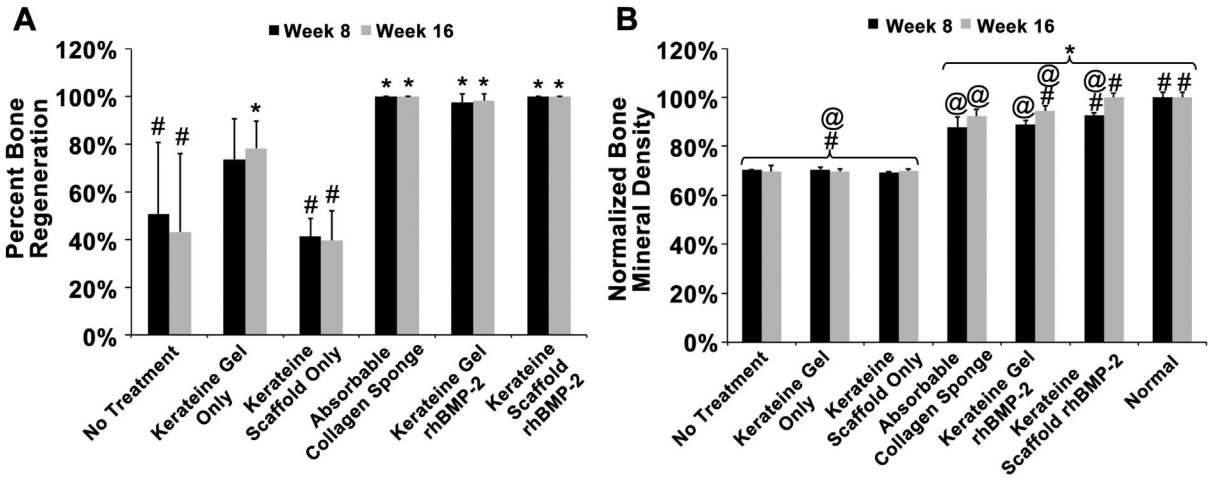

Fig. 5.

(A) Bone regeneration was normalized to initial defect volume with complete defect bridging represented by 100%. (B) Regenerated bone mineral density of the defect area was normalized to normal uninjured bone at the same location. (n = 5 animals with bilateral treatment averaging, Mean ± SD; *p < 0.0001 vs No Treatment, #p < 0.05 vs ACS, @p < 0.0001 vs Normal Bone).

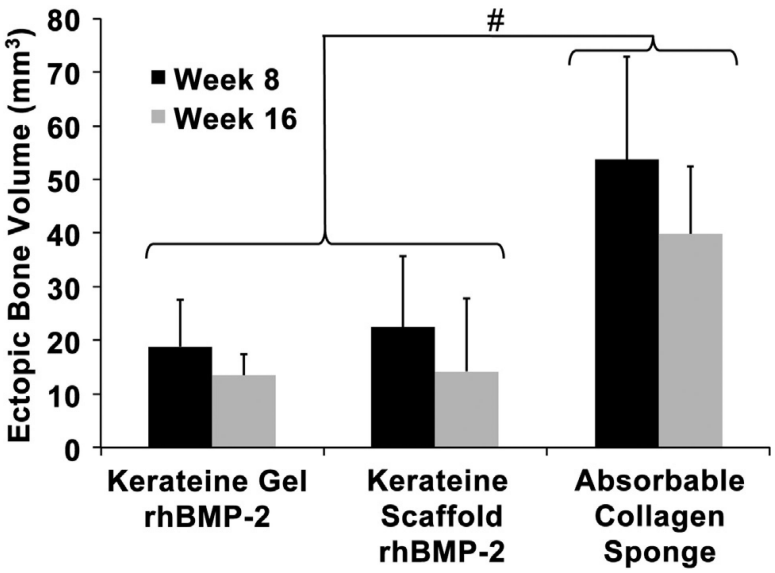

Fig. 6.

Ectopic bone growth volume for rhBMP-2 carrier system as determined by volumetric analysis of μCT images. (n = 5 animals with bilateral treatment averaging; Mean ± SD; #p < 0.0001 vs ACS).

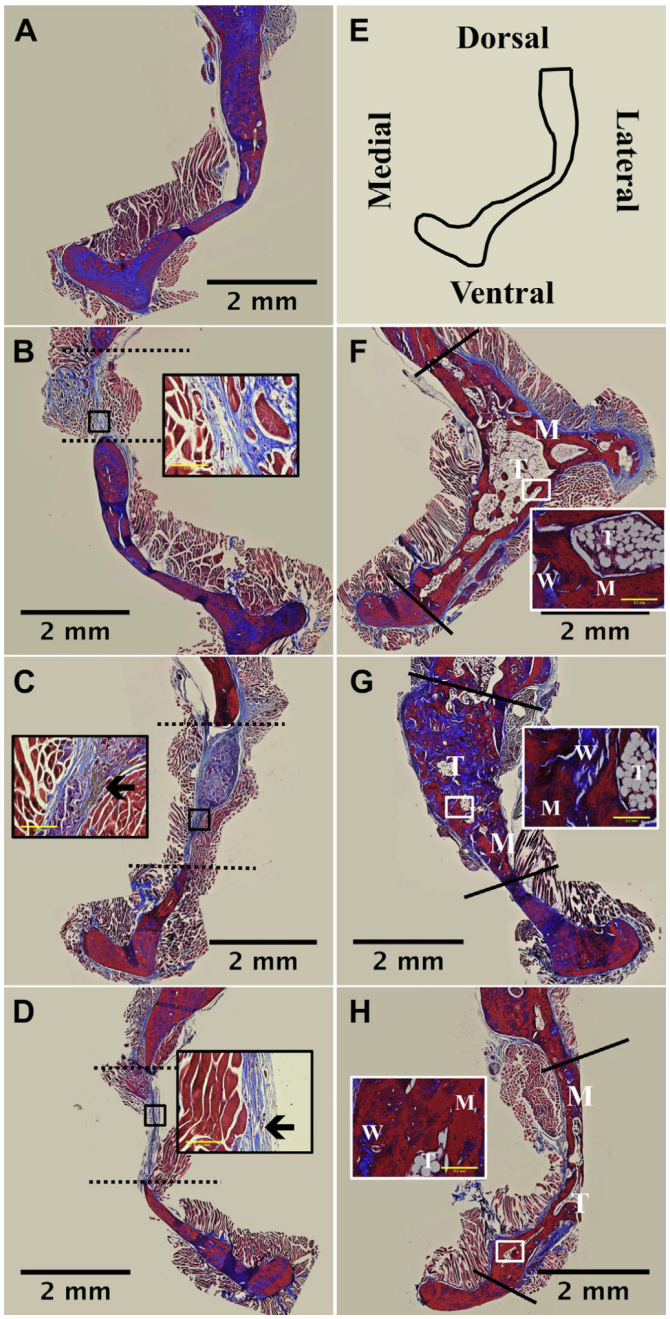

Fig. 7.

Histological images of bone regeneration in section of rat hemi-mandibles 16 weeks post-surgery. Mandibles were sectioned along the coronal plane of the decalcified defect area and stained with Masson's Trichrome. (A) Normal bone and (E) a schematic of the anatomical orientation. Animals administered (B) no treatment, (C) kerateine scaffold, or (D) kerateine gel without rhBMP-2 were unable to bridge the defect (indicated by dashed line). (F) Absorbable collagen sponge, (G) kerateine scaffold, or (H) kerateine gel loaded with 5 μg rhBMP-2 were able to close the defect (solid line) with mature (M), woven (W) and trabecular (T) bone. Each main image is stitched from images collected with a 4× objective;

scale bar denotes 2 mm. For B, C, D, F, G, and H insets are images taken with 20× objective (scale bar indicates 0.2 mm). Insets for no treatment (B) and kerateine carriers without rhBMP-2 (C &D) highlight the collagen fiber orientation as well as remaining kerateine carrier after 16 weeks (arrows). Insets for rhBMP-2 treatment groups highlight varying stages of bone formation.